European Journal of Pharmaceutical Sciences 82 (2016) 161–170

Contents lists available at ScienceDirect

European Journal of Pharmaceutical Sciences

journal homepage: www.elsevier.com/locate/ejps

Quercetin derivatives as novel antihypertensive agents: Synthesis and physiological characterization

Fedora Grande [a,1], Ortensia I. Parisi [a,b,1], Roberta A. Mordocco [a], Carmine Rocca [c], Francesco Puoci [a,*], Luca Scrivano [a], Anna M. Quintieri [c], Patrizia Cantafio [c], Salvatore Ferla [d], Andrea Brancale [d], Carmela Saturnino [e], Maria C. Cerra [c,*], Maria S. Sinicropi [a,2], Tommaso Angelone [c,2]

[a] Department of Pharmacy, Health and Nutritional Sciences, University of Calabria, 87036 Arcavacata di Rende, CS, Italy
[b] Department of Informatics, Modeling, Electronics and Systems Engineering, University of Calabria, 87036 Arcavacata di Rende, CS, Italy
[c] Department of Biology, Ecology and E.S., University of Calabria, 87036 Arcavacata di Rende, CS, Italy
[d] School of Pharmacy and Pharmaceutical Sciences, Cardiff University, Wales, UK
[e] Department of Pharmaceutical and Biomedical Sciences, University of Salerno, 84084 Fisciano, SA, Italy

ARTICLE INFO

Article history:
Received 29 July 2015
Received in revised form 6 November 2015
Accepted 25 November 2015
Available online 02 December 2015

Keywords:
Quercetin
Heart
Hypertension
Nitric oxide

ABSTRACT

The antihypertensive flavonol quercetin (**Q1**) is endowed with a cardioprotective effect against myocardial ischemic damage. **Q1** inhibits angiotensin converting enzyme activity, improves vascular relaxation, and decreases oxidative stress and gene expression. However, the clinical application of this flavonol is limited by its poor bioavailability and low stability in aqueous medium.

In the aim to overcome these drawbacks and preserve the cardioprotective effects of quercetin, the present study reports on the preparation of five different **Q1** analogs, in which all OH groups were replaced by hydrophobic functional moieties.

Q1 derivatives have been synthesized by optimizing previously reported procedures and analyzed by spectroscopic analysis. The cardiovascular properties of the obtained compounds were also investigated in order to evaluate whether chemical modification affects their biological efficacy. The interaction with β-adrenergic receptors was evaluated by molecular docking and the cardiovascular efficacy was investigated on the ex vivo Langendorff perfused rat heart. Furthermore, the bioavailability and the antihypertensive properties of the most active derivative were evaluated by in vitro studies and in vivo administration (1 month) on spontaneously hypertensive rats (SHRs), respectively.

Among all studied **Q1** derivatives, only the ethyl derivative reduced left ventricular pressure (at 10^{-8} M ÷ 10^{-6} M doses) and improved relaxation and coronary dilation. NOSs inhibition by L-NAME abolished inotropism, lusitropism and coronary effects. Chronic administration of high doses of this compound on SHR reduced systolic and diastolic pressure. Differently, the acetyl derivative induced negative inotropism and lusitropism (at 10^{-10} M and 10^{-8} ÷ 10^{-6} M doses), without affecting coronary pressure. Accordingly, docking studies suggested that these compounds bind both β1/β2-adrenergic receptors.

Taking into consideration all the obtained results, the replacement of OH with ethyl groups seems to improve **Q1** bioavailability and stability; therefore, the ethyl derivative could represent a good candidate for clinical use in hypertension.

© 2015 Published by Elsevier B.V.

1. Introduction

Quercetin (**Q1**) is the major representative of flavonols, a subclass of flavonoids (Fig. 1). This compound is often present in glycosylated form, the associated sugar moiety is usually glucose and, although glycosylation can occur at any of the five hydroxyl groups, the most common quercetin glycoside presents the sugar moiety appended at position 3 (isoquercetin).

The major sources of **Q1** are fruits such as apples, citrus, berries and cherries, vegetables such as onions and broccoli, and beverages such as red wine and tea (Kaur and Kapoor, 2001). It has been also found in several medical plants, such as *Ginkgo biloba*, *Aesculus hippocastanum* and *Hypericum perforatum* (Sharma and Gupta, 2010). The interest towards this flavonol is due to its wide range of bioactivity. **Q1** shows not only antioxidant properties like all the flavonoids (Hayek et al., 1997) but also anti-inflammatory (Ferry et al., 1996), antiviral, antibacterial,

* Corresponding authors.
E-mail addresses: francesco.puoci@unical.it (F. Puoci), maria_carmela.cerra@unical.it (M.C. Cerra).
[1] These authors have contributed equally to the manuscript.
[2] Co-senior authors.

http://dx.doi.org/10.1016/j.ejps.2015.11.021
0928-0987/© 2015 Published by Elsevier B.V.

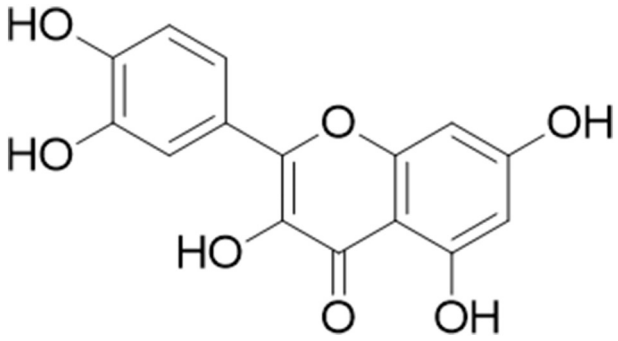

Fig. 1. Chemical structure of quercetin.

anticarcinogenic (Deschner et al., 1991; Pereira et al., 1996; Verma et al., 1988), liver-protecting, cardiovascular (Angelone et al., 2011; Pérez-Vizcaíno et al., 2002) and anti-platelet effects (Pignatelli et al., 2000).

Inhibition of cardiac voltage-gated sodium channels (VGSCs) is antiarrhythmic and cardioprotective (Catalano et al., 2013; Carocci et al., 2010). Quercetin, as well as other polyphenols, possesses structural similarities to several antiarrhythmic VGSC inhibitors, contributing to its cardioprotection (Wallace et al., 2006).

The mechanisms by which quercetin exerts these effects are not completely understood, but it is plausible that different biochemical processes are involved. For example, the antioxidant properties seem to be due to the ability of **Q1** to act as a scavenger of free radicals and bind transition metals. This capability makes **Q1** able to inhibit lipid peroxidation and protect cell membranes and nucleic acids from the free radical-mediated molecular damages.

Several recent studies focused on the **Q1** cardiovascular protective effects. In particular, the antihypertensive effect of such a flavonol has been extensively studied. This compound resulted able to decrease oxidative stress, inhibit angiotensin converting enzyme activity, improve endothelium vascular relaxation, and modulate cell signaling and gene expression (Angelone et al., 2011; Larson et al., 2010; Pignatelli et al., 2000).

However, the clinical application of **Q1** is limited by its poor bioavailability and low stability in aqueous medium, due in particular to the two phenolic hydroxyl groups at positions 3 and 7 (Campiglia and Pezzi, 2013).

During the last years, several studies have been carried out to enhance the pharmacokinetic properties and chemical stability of **Q1** and numerous derivatives, showing different biological properties, have been identified (Kim et al., 2010).

Based on the results obtained in our previous study, which demonstrated that quercetin is able to induce biphasic inotropic and lusitropic effects, herein we describe the preparation of five different **Q1** derivatives in which OH groups have been replaced with hydrophobic functional groups in the aim to enhance the lipophilic character of this compound and, thus, improve its bioavailability.

All the synthesized molecules have been subjected to in vitro tests to estimate their bioavailability and in vivo assays to evaluate the cardiovascular effects.

2. Materials and methods

2.1. Chemistry

2.1.1. General chemical information

Melting points were determined using a Veego make silicon oil bath-type melting point apparatus and are uncorrected. Purity of the compounds and completion of reactions were monitored by thin layer chromatography (TLC) on silica gel plates (60 F_{254}; Merck), visualizing with ultraviolet light or iodine vapors. The IR spectra were recorded using KBr disk method on a Shimadzu FT-IR, Model 8300. The ^{1}H NMR spectra (on a Bruker 300/400 MHz spectrometer) were recorded in DMSO. Chemical shifts were reported as part per million (δ ppm) using tetramethylsilane (TMS) as an internal standard. The assignment of exchangeable protons was confirmed by the D_2O exchange studies wherever required. Mass spectral data was obtained on a QTRAP Applied Biosystem SCIEX spectrometer or on JEOL-SX-102 instrument (JEOL, Tokyo, Japan) by fast atom bombardment (FAB positive mode). Spectral data (IR and NMR) confirmed the structures of the synthesized compounds and the purity was ascertained by microanalysis.

2.1.2. 2-(3,4-Diacetoxyphenyl)-4-oxo-4H-chromene-3,5,7-triyl triacetate (**Q2**)

This compound was synthesized following experimental conditions previously described (Picq et al., 1982).

The crude resulting was purified by column chromatography (chloroform/ethyl acetate, 9:1 as solvent). The product was isolated as a white solid, 35% yield. Mp 190 °C (chloroform/ethyl acetate). ^{1}H NMR ($CDCl_3$) δ: 7.54–7.50 (m, 2H), 7.31–7.02 (m, 2H), 6.56 (d, 1H, J = 2.1 Hz), 2.42–2.15 (m, 15H).^{13}C NMR ($CDCl_3$) δ: 169.25, 167.81, 167.74, 156.85, 154.25, 150.41, 144.37, 142.19, 127.77, 126.42, 123.92, 123.84, 113.88, 108.96, 21.17, 21.02, 20.65, 20.50. IR υ_{max}: 1775, 1645, 1178, 1149, 1127, 1107, 1074, 1021, 899 cm^{-1}.

2.1.3. 2-(2,2-Diphenylbenzo[d][1,3]dioxol-5-yl)-3,5,7-trihydroxy-4H-chromen-4-one (**Q3**)

This compound was prepared according to an experimental procedure previously described (Lu et al., 2014).

The crude resulting oil was purified by column chromatography (petroleum ether/ethyl acetate, 4:1 as solvent). The product was isolated as a yellow solid, 7% yield. Mp 217 °C (petroleum ether/ethyl acetate). ^{1}H NMR (d_6-acetone) δ: 12.0 (s br, 3H, OH); 7.76 (m, 2H); 7.50 (m, 3H); 7.38–7.23 (m, 6H); 7.09–6.98 (m, 1H); 6.42 (d, 1H); 6.15 (d, 1H). ^{13}C NMR ($CDCl_3$) δ: 175.13, 162.26, 161.13, 156.2, 148.89, 147.60, 139.76, 135.68, 129.33, 128.48, 127.51, 126.25, 125.40, 124.53, 122.95, 108.67, 107.90, 103.82, 98.84, 94.11. IR υ_{max}: 2800, 1598, 1493, 1260, 1241, 1213, 1187, 1043, 1018, 697 cm^{-1}.

2.1.4. 2-(2,2-Diphenylbenzo[d][1,3]dioxol-5-yl)-4-oxo-4H-chromene-3,5,7-triyl triacetate (**Q4**)

This compound was synthesized following experimental conditions previously described (Kim et al., 2010).

The product was isolated as a white solid, 32% yield. Mp 193 °C (chloroform/ethyl acetate). ^{1}H NMR (d_6-acetone) δ: 7.53–7.31 (m, 5H, Ar); 7.39–7.29 (m, 5H, Ar); 7.07 (m, 3H); 6.88 (m, 2H); 2.22 (m, 9H). ^{13}C NMR ($CDCl_3$) δ: 170.09, 169.30, 167.84, 156.81, 155.24, 154.05, 150.33, 149.80, 147.68, 139.53, 129.42, 128.43, 128.41, 128.40, 128.38, 128.36, 128.35, 128.33, 128.26, 126.26, 126.25, 126.23, 126.21, 126.18, 123.53, 123.04, 114.69, 113.65, 108.87, 108.74, 108.28, 21.18, 21.05, 20.66. IR υ_{max}: 1777, 1626, 1496, 1259, 1176, 1138, 1043, 1019, 754 cm^{-1}.

2.1.5. 2-(3,4-Diethoxyphenyl)-3,5,7-triethoxy-4H-chromen-4-one (**Q5**)

This compound was prepared according to an experimental procedure previously described (Picq et al., 1982).

The product was isolated as a yellow solid, 20% yield. Mp 123 °C (n-hexane–chloroform/ethyl acetate). ^{1}H NMR ($CDCl_3$) δ: 7.78–7.58 (m, 2H, Ar); 7.03–6.83 (m, 2H, Ar); 6.34 (m, 1H); 4.28–3.86 (m, 10H); 1.92–1.09 (m, 12H), 0.89–0.75 (m, 3H). ^{13}C NMR ($CDCl_3$) δ: 178.90, 164.74, 161.97, 156.73, 151.07, 148.09, 137.85, 122.98, 122.10, 113.57, 112.17, 111.05, 98.09, 92.56, 68.56, 68.03, 64.42, 64.17, 29.68, 15.70, 15.62, 14.80, 14.69, 14.56. IR υ_{max}: 1599, 1474, 1393, 1267, 1214, 1172, 749 cm^{-1}.

*2.1.6. 3,5,7-Tris(benzyloxy)-2-(3,4-bis(benzyloxy)phenyl)-4H-chromen-4-one (**Q6**)*

This compound was prepared according to an experimental procedure previously described (Bouktaib et al., 2002).

The product was isolated as a yellow solid, 15% yield. Mp 121 °C (dichloromethane).^{1}H NMR ($CDCl_3$) δ: 7.68–7.50 (m, 4H), 7.40–7.08 (m, 23H); 6.9–6.79 (m, 1H); 6.45–6.28 (m, 2H); 5.19–4.89 (m, 10H). ^{13}C NMR ($CDCl_3$) δ: 178.82, 164.44, 162.02, 156.66, 156.30, 147.81, 145.56, 137.60, 137.44, 136.88, 136.63, 136.42, 135.78, 135.64, 128.84, 128.78, 128.73, 128.67, 128.60, 128.49, 128.33, 128.27, 128.18, 128.01, 127.86, 127.45, 127.33, 127.16, 123.95, 123.43, 122.59, 121.88, 115.26, 114.86, 113.62, 111.53, 106.20, 98.64, 92.98, 74.34, 74.22, 71.11, 70.84, 70.41. IR υ_{max}: 1586, 1255, 1194, 1166, 1123, 1001, 815 cm^{-1}.

2.2. Molecular modeling and docking simulations

The molecular modeling simulations were performed on an Apple Mac pro 2.66 GHz Quad-Core Intel Xeon, Running Ubuntu 12.04. Different crystal structures of human β2-adrenergic receptors were examined in order to identify the putative binding site. The β2-adrenergic receptor bound to the partial agonist carazol (PDB ID: 2RH1) was chosen for our docking studies (Cherezov et al., 2007).

No human crystal structure of the β1-adrenergic receptor is available, so the *Meleagris gallopavo* β1 receptor co-crystallized with the partial agonist cyanopindolol has been used (PDB ID: 4BVN) (Miller-Gallacher et al., 2014). Due to the high identity with the human β1-adrenergic receptor (75% identity) and the conserved amino acids residues of the binding site, no homology model preparation was required and the crystal structure was used for the docking studies.

Docking studies were performed using Glide docking as part of Maestro package (Glide, Maestro version 9.5.014, Schrödinger, Inc., New York, NY).The two co-crystallized molecules were selected as center of the binding site and, then, the selection was extended to the near amino acids building a 12 **Å** grid. A ligands database in Maestro format, prepared using the LigPrep function, was used as input for the docking calculation. Ligand docking was performed using Glide SP (standard precision) setting the default values, and no water molecules were considered. The output solutions were visual inspected in MOE to identify the interaction between ligand and protein (Molecular Operating Environment,http://www.chemcomp.com/MOE-Molecular_Operating_Environment.htm, accessed Aug. 20, 2014).

2.3. Bioavailability studies

2.3.1. General bioavailability methods

Hydrochloric acid, pepsin from porcine gastric mucosa, esterase from porcine liver, α-amylase from porcine pancreas, pancreatin from porcine pancreas, sodium cholate, sodium dihydrogen phosphate, disodium hydrogen phosphate and sodium hydrogen carbonate were purchased by Sigma-Aldrich (Sigma Chemical Co., St. Louis, MO, USA). All solvents were reagent-grade or HPLC-grade and provided by Carlo Erba Reagents (Milano, Italia). Dialysis tubes were provided by Spectrum Laboratories Inc., MWCO: 12–14,000 Da, U.S.A. Absorption spectra were recorded with a Jasco V-530 UV/Vis spectrometer.

2.3.2. In vitro bioavailability studies

In vitro bioavailability studies were carried out in simulated gastric and intestinal fluids through a slight modified dialysis tubing procedure (Chimento et al., 2013). The dialysis tubing method is based on two enzymatic phases: pepsin digestion, which occurs in the first 2 h, and pancreatin digestion, in the following 4 h. The two phases are described below.

2.3.2.1. Pepsin digestion. 300 μL of a **Q5** solution (1.0 mM in DMSO) were mixed with 1.0 mL of a 0.85 N HCl solution containing 24,000 U of porcine pepsin per mL and 3.0 mL of a sodium cholate solution (2% *w*/*v* in distilled water). The obtained mixture was introduced into a dialysis bag, which was sealed on each end with clamps and immersed in a flask containing 10 mL of a 0.85 N HCl solution (pH 1.0). The flask was then incubated for 2 h into a shaking water bath at 37 ± 0.5 °C, simulating the human physiological conditions of temperature.

2.3.2.2. Pancreatin digestion. At the end of the 2 h pepsin digestion, the dialysis bag was recovered and carefully opened. 11 mg of amylase, 11 mg of esterase and 1.3 mL of a 0.8 M $NaHCO_3$ solution containing 22.60 mg porcine pancreatin/mL were added to the peptic digesta. After the digesta and enzymes solution were mixed, the dialysis bag was sealed again and placed into a flask with 10 mL of a phosphate buffer solution at pH 7.0. The flask was incubated into the shaking water bath at 37 ± 0.5 °C for further 4 h.

In order to evaluate the in vitro bioavailability of the sample, 3 mL of the medium were withdrawn from the flask at the time points of 2 and 6 h, after pepsin and pancreatin digestions, respectively. The concentrations of the samples were determined by UV/Vis spectroscopy and calculated by using the equations obtained from the calibration curves of **Q5** standard solutions at pH 1.0 and 7.0, respectively. For this purpose, all the prepared standard solutions were analyzed by UV–vis spectrophotometer and the correlation coefficient (R^2) and slope of the regression equations obtained by the method of least square were calculated at pH 1.0 and 7.0, respectively.

The same procedure was applied to evaluate the bioavailability of **Q1**, used as control for data confrontation.

Each experiment was repeated three times.

2.4. In vivo studies

2.4.1. Animals

Animal care, sacrifice and experiments were in accordance with the Italian law (D.L. 26/2014), the Guide for Care and Use of Laboratory Animals published by the US National Institutes of Health (2011), and the Directive 2010/63/EU of the European Parliament on the protection of animals used for scientific research.

2.4.2. Perfusion technique

The performance of the rat heart was evaluated according to the Langendorff technique (Angelone et al., 2015). Rats were anesthetized with ethyl carbamate (2 g/kg rat, i.p.). Hearts were rapidly excised and transferred in ice-cold buffered Krebs–Henseleit solution (KHS). Aorta was immediately cannulated with a glass cannula and connected with the Langendorff apparatus to start perfusion at a constant flow-rate of 12 mL/min in order to avoid fluid accumulation, the apex of the left ventricle (LV) was pierced. A water-filled latex balloon, connected to a BLPR gauge (WRI, Inc. USA), was inserted through the mitral valve into the LV to allow isovolumic contractions and to continuously record mechanical parameters. The balloon was progressively filled with water up to 80 μL to obtain an initial left ventricular end diastolic pressure of 5–8 mm Hg. Coronary pressure was recorded using another pressure transducer located just above the aorta.

Left ventricular pressure (LVP) was measured by means of a latex water-filled balloon inserted into the left ventricle via the left atrium [adjusted to obtain left ventricular end-diastolic pressure (LVEDP) of 5–7 mm Hg] and connected to a pressure transducer (BLPR gauge; WRI, USA). The maximal values of the first derivative of LVP, [+(LVdP/dt) max, mm Hg/s], which indicates the maximal rate of left ventricular contraction, the maximal rate of left ventricular pressure decline of LVP [(LVdP/dt) min, mm Hg/s], the rate pressure product (RPP: HR LVP, in 10^4 mm Hg beats/min), used as an index of cardiac work, and LVEDP were used to assess cardiac function.

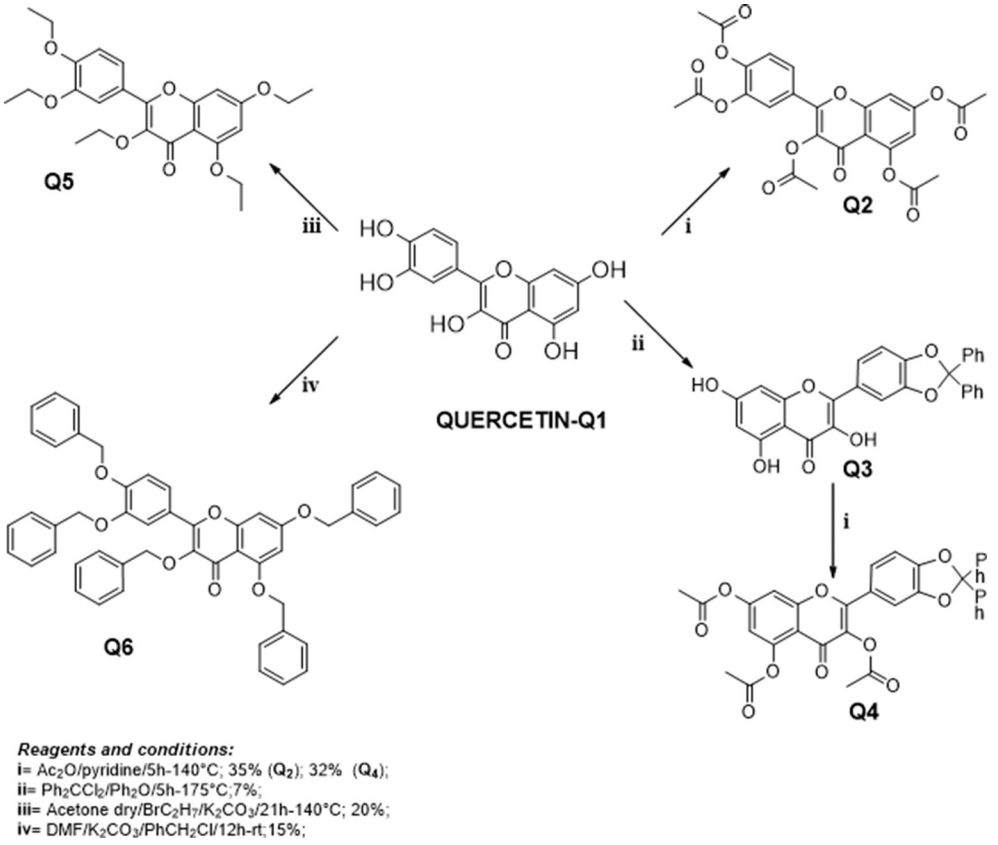

Scheme 1. Reagents and reaction conditions for **Q1** derivatives synthesis.

Mean coronary pressure (CP, mm Hg) was calculated as the average of values obtained during several cardiac cycles.

The perfusion solution consisted of a modified non recirculating KHS containing 113 mM NaCl, 4.7 mM KCl, 25 mM $NaHCO_3$, 1.2 mM $MgSO_4$, 1.8 mM $CaCl_2$, 1.2 mM KH_2PO_4, 11 mM glucose, 1.1 mM mannitol, 5 mM Na-pyruvate. pH was adjusted to 7.4 with NaOH (1 M) and the solution was equilibrated at 37 °C by 95% O_2–5% CO_2. All drug-containing solutions were freshly prepared before the experiments.

2.4.2.1. Statistics. Statistical analysis was performed by one-way ANOVA and Newman–Keuls Multiple Comparison Test, when appropriate. Differences were considered statistically significant at $P < 0.05$. GraphPad Prism software, version 5 (GraphPad Software, San Diego, CA) will be used for all the statistical analysis.

2.4.3. Drug-stimulated preparations

For each drug, preliminary experiments (data not shown) obtained by the repetitive exposure of each heart to one concentration of the single drug (10^{-8} M) revealed the absence of desensitization. Thus, concentration-response curves were generated by perfusing each cardiac preparation with KHS enriched with increasing concentrations of either **Q2**, or **Q3**, or **Q4**, or **Q5**, or **Q6**, or **Q1** (from 10^{-10} M to 10^{-6} M) for 10 min.

3. Results and discussion

3.1. Chemical

The preparation of five **Q1** derivatives, in which all the OH groups have been substituted with different hydrophobic functional groups, has been performed optimizing previously reported procedures as depicted in Scheme 1 (Kim et al., 2010; Lu et al., 2014; Picq et al., 1982).

3.2. Molecular docking studies

A series of molecular docking studies were performed to investigate the putative binding mode of the reported compounds on both β1 and β2 receptors. Quercetin (**Q1**) seems able to bind both receptors (Fig. 2). In the β2-receptor **Q1** forms two H-bonds with Asp113, while in the β1 it establishes three different H-bonds (Asn129,

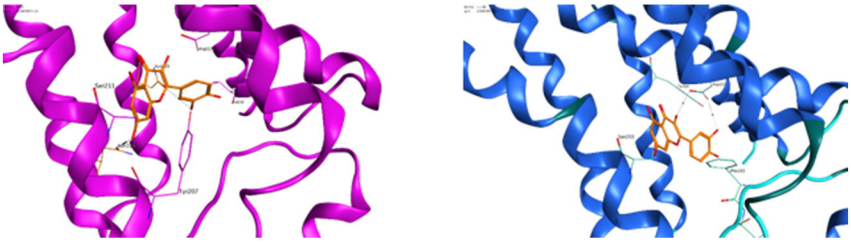

Fig. 2. Q1 docked in the β1 (purple) and β2-adrenergic (blue) receptors. (For interpretation of the references to color in this figure legend, the reader is referred to the web version of this article.)

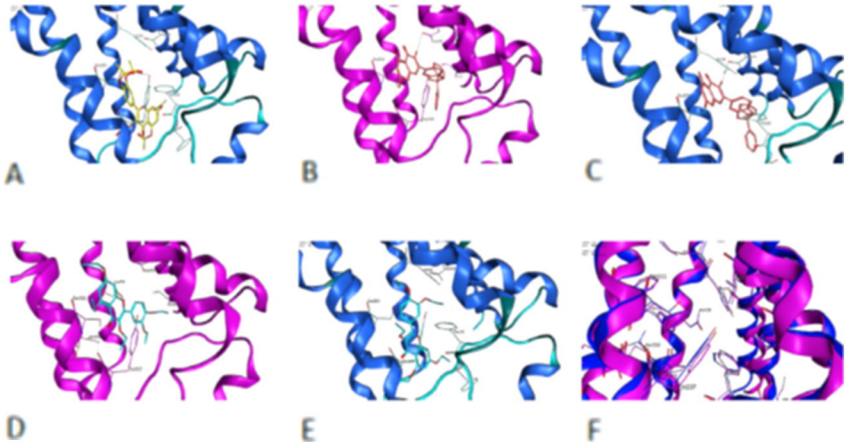

Fig. 3. **Q2** docked in the β2-adrenergic receptor (A). **Q3** docked in the β1- (B) and β2-adrenergic (C) receptors. **Q5** docked in the β1- (D) and β2-adrenergic (E) receptors. Superposition of the β2 (blue) and β1 (purple) active sites (F). (For interpretation of the references to color in this figure legend, the reader is referred to the web version of this article.)

Tyr207, Asn319). The possibility to bind both receptors could lead to β1/β2-adrenergic biological effects caused by quercetin.

Interestingly, compounds **Q4** and **Q6** could not be docked in any of the receptors, probably because of their rigidity and steric hindrance. This observation could possibly explain the total absence of activity for **Q6** and the very small activity for **Q4**. Compound **Q2** gave good docking results only for the β2-receptor (Fig. 3A) interacting with Tyr199 and occupying the active site as **Q1**. Once again, we could not generate any useful docking result from the β1-receptor. **Q3** and **Q5** docks well with both receptors. **Q3** forms H-bonds with Aps121 and Ser211 in the β1 and with Asp113 and Ser203 in the β2 (Fig. 3B, C). **Q5** does not seem to establish any specific hydrogen bond but it occupies extensively the active site (Fig. 3D, E).

From these studies, we can say that **Q1** and the other most active compounds **Q2**, **Q3** and **Q5,** could potentially interact with the β-adrenergic receptors. Due to the similar active site geometry (Fig. 3F) between the two types of β-receptors, it is likely that the reported compounds can easily bind both targets balancing the different biological effects linked with the specific β-adrenergic receptors.

3.3. Ex vivo studies

3.3.1. Basal conditions

After 20 min of stabilization, the following basal recordings were measured: LVP = 85 ± 1.7 mm Hg, heart rate (HR) = 276 ± 7.3 beats/min, RPP = 3.3 ± 0.12 10^4 mm Hg beats/min, CP = 66 ± 1.7 mm Hg, +(LVd*P*/d*T*) max = 2768 ± 82.1 (mm Hg/s) and-(LVd*P*/d*T*) max = 1547 ± 28.7 (mm Hg/s).

Endurance and stability of the preparation, analyzed by measuring performance variables every 10 min, showed that the heart preparation is stable for up to 180 min on the perfusion apparatus.

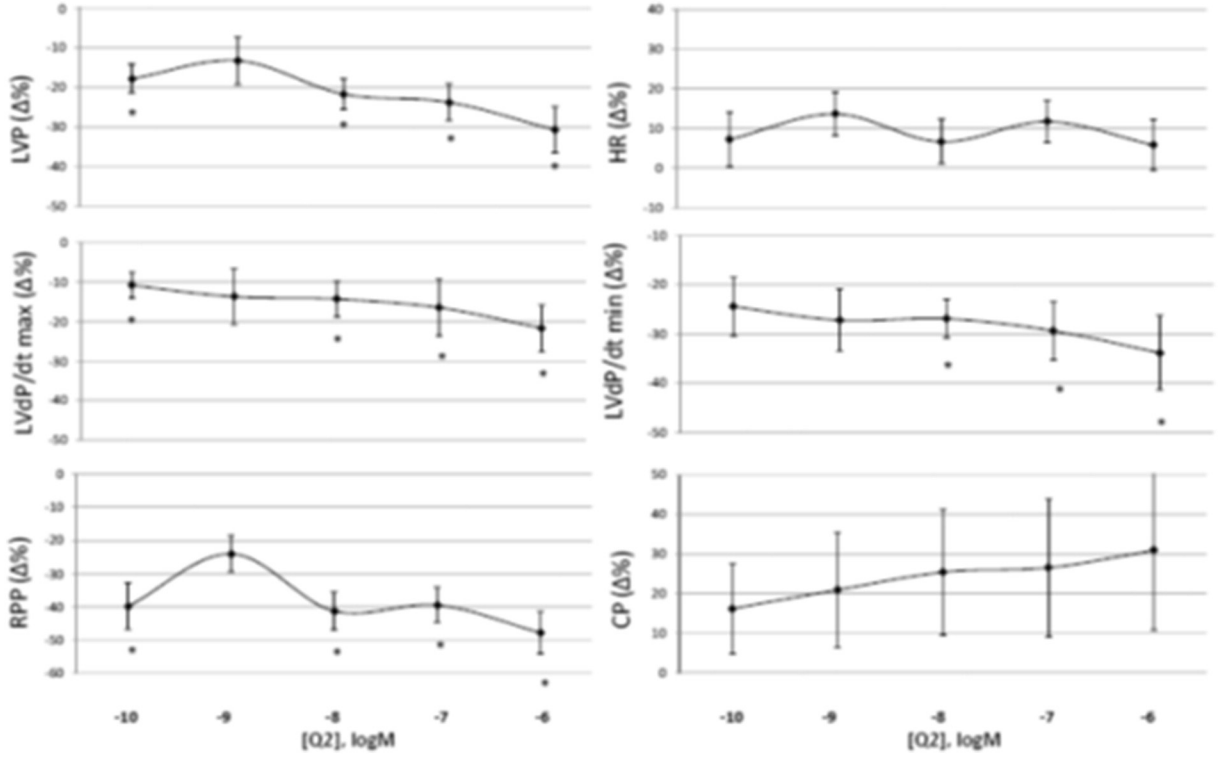

Fig. 4. Dose-dependent response curves of **Q2** (10^{-10} M–10^{-6} M) on LVP, HR, (LVd*P*/d*T*) max, (LVd*P*/d*T*) min, RPP and CP, on Langendorff perfused rat heart preparations. Percentage changes were evaluated as means ± SEM of 7 experiments. Significance of difference from control values was evaluated by one-way ANOVA; $P = 0 < 0.05$.

*3.3.2. Dose–response curves of **Q1–Q6***

The biological efficacy of **Q1** and its modified derivatives was evaluated by analyzing the hemodynamic performance of the rat heart *ex vivo* perfused according to Langendorff. We found that application of **Q1** from 10^{-10} M to 10^{-6} M resulted in positive inotropic and lusitropic effects at low concentrations (10^{-10} to 10^{-8} M) and in negative inotropic and lusitropic effects at higher concentrations (10^{-7} and 10^{-6} M). **Q1** induced vasodilation at low concentration (10^{-10} to 10^{-8} M) while it did not modify HR (data not shown). These effects are similar to those previously published by Angelone et al. (2011). **Q2** determined a significant negative inotropic effect revealed by the reduction of LVP, LVd*P*/d*t* max and RPP, and a negative lusitropic effect revealed by the reduction of LVd*P*/d*t* min. **Q2** did not significantly affect HR, while it induced vasoconstriction at all concentrations tested (Fig. 4). Contrarily, **Q3** was unable to affect the rat cardiac performance, except for a small vasoconstriction detected at high concentration (10^{-7} M) (Fig. 5). **Q4** exposure induced a decrease in LVP and LVd*P*/d*t* max at 10^{-6} M, while it unchanged the other cardiac parameters (Fig. 6). Notably, **Q5** induced a dose-dependent significant negative inotropic effect revealed by the reduction of LVP, LVd*P*/d*t* max and RPP, and a negative lusitropic effect revealed by the reduction of LVd*P*/d*t* min (Fig. 4). **Q5** did not change HR, but it determined a significant reduction of the coronary pressure at high concentrations (from 10^{-8} M to 10^{-6} M) (Fig. 7). **Q6** did not affect the cardiac performance (Fig. 8).

*3.4. Cellular mechanism of action of **Q5***

In the present study, we analyzed the transduction pathway activated by **Q5** since, contrary to all others quercetin derivatives here tested, it induces a coronary vasodilation which is significant at high doses. This coronary effect is similar to that elicited by quercetin on the *ex vivo* rat heart, already shown by Angelone et al. (2011), and resembles the coronary activity of flavonols (Duarte et al., 1993, 2001). It has been reported in the mammalian heart, that β1- and β2-adrenoceptors represent the main intermediaries of the cardiac response to adrenergic stimulation, each of them modulates different signal pathways resulting in different outcomes on cardiac function. β1-adrenoceptor, the most abundant subtype in mammalian heart (Brodde et al., 2006), induces the activation of the stimulatory G protein (Gαs)/adenylyl cyclase (AC)/cAMP/cAMP-dependent protein kinase A (PKA) pathway (Woo and Xiao, 2002), while β2-adrenoceptor has been shown to regulate an alternative signaling through the activation of inhibitory G proteins (Gαi) (Woo and Xiao, 2002). The main signal pathway regulated by β2-adrenoceptors through Gαi is the phosphatidylinositol-3 kinase (PI3K) signaling cascade and the activation of the Nitric Oxide pathway (Conti et al., 2013). Our docking studies indicated that **Q5** binds both β1- and β2-adrenergic receptors. However, since **Q5** determined negative inotropism, lusitropism and vasodilation, we suggest that it mainly interacts with β2 adrenergic receptor. In order to explore the intracellular β2-dependent mechanism of action by which **Q5** determines negative inotropism and lusitropism and vasodilation, hearts were treated with the NOSs inhibitor L-NAME in the presence of **Q5** (Fig. 9). Results indicated that L-NAME abolished **Q5**-dependent cardiac effects suggesting the obligatory role of NO in mediating the intracellular signaling activated by this derivative.

3.5. In vitro bioavailability studies

Most of the natural compounds suffer of low *in vivo* bioavailability. Possible reasons for a reduced bioavailability are low intrinsic activity, low degree of absorption, high metabolization rate, poor activity of metabolites and/or rapid elimination (Bhattaram et al., 2002). Despite its strong activity, several studies in the past decades related the low bioavailability of **Q1** to poor absorption and rapid metabolism (Cai et al., 2013).

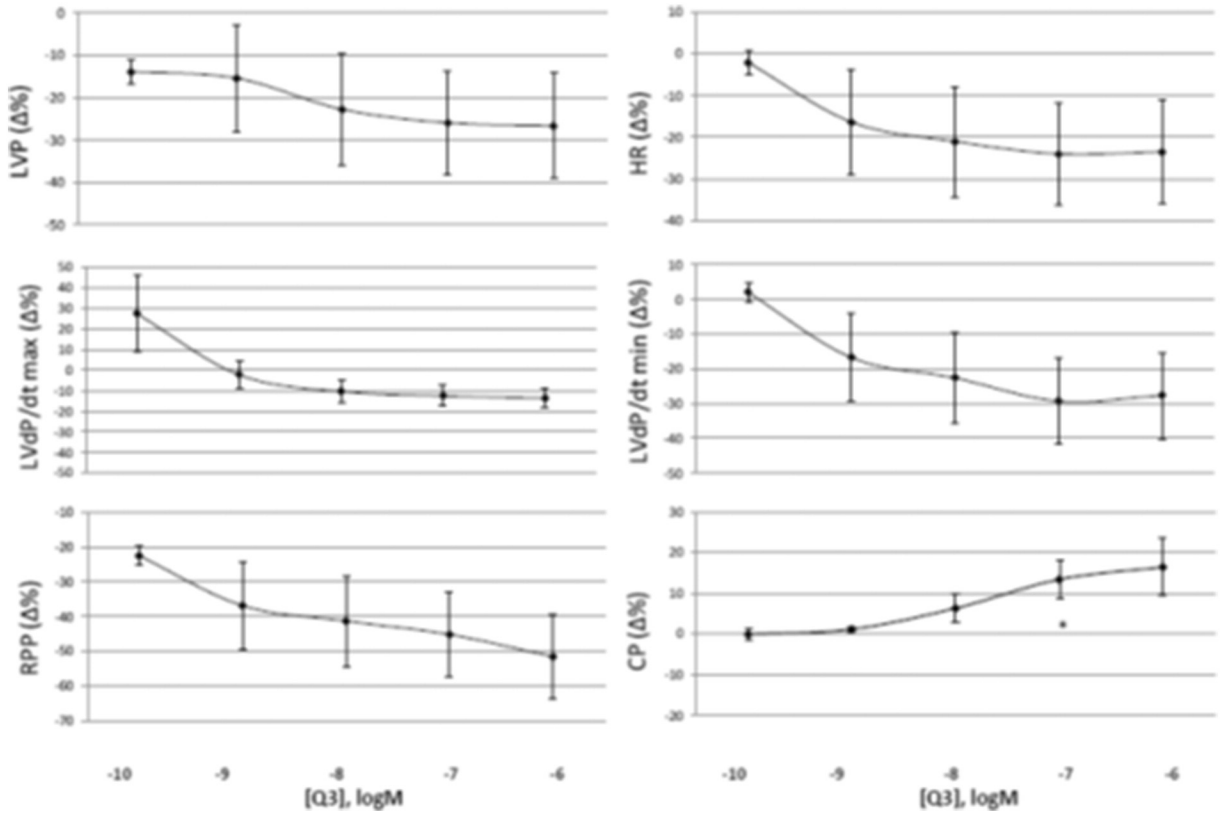

Fig. 5. Dose-dependent response curves of **Q3** (10^{-10} M–10^{-6} M) on LVP, HR, (LVd*P*/d*T*) max, (LVd*P*/d*T*) min, RPP and CP, on Langendorff perfused rat heart preparations. Percentage changes were evaluated as means ± SEM of 7 experiments. Significance of difference from control values was evaluated by one-way ANOVA; $P = 0 < 0.05$.

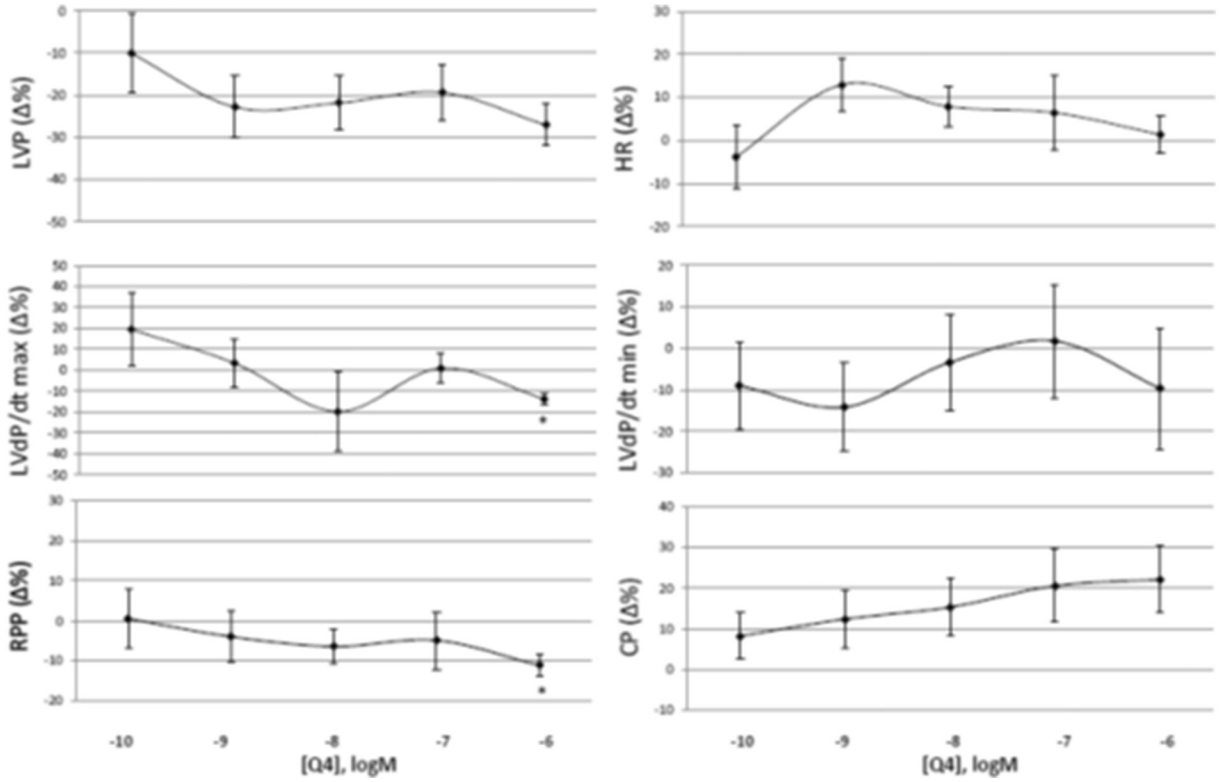

Fig. 6. Dose-dependent response curves of **Q4** (10^{-10} M–10^{-6} M) on LVP, HR, LVd*P*/d*T* max, LVd*P*/d*T* min, RPP and CP, on Langendorff perfused rat heart preparations. Percentage changes were evaluated as means ± SEM of 7 experiments. Significance of difference from control values was evaluated by one-way ANOVA; $P = 0 < 0.05$.

In the attempt to improve **Q1** bioavailability, several molecular modifications could be introduced. Considering the hydrophilic/hydrophobic ratio of the molecule, most of the hydrophilic character of **Q1** is provided by –OH groups. In order to improve its hydrophobicity, as well as its capability to cross biological membranes, the modification of these groups in more hydrophobic ones is an interesting strategy. Indeed, the ethylation

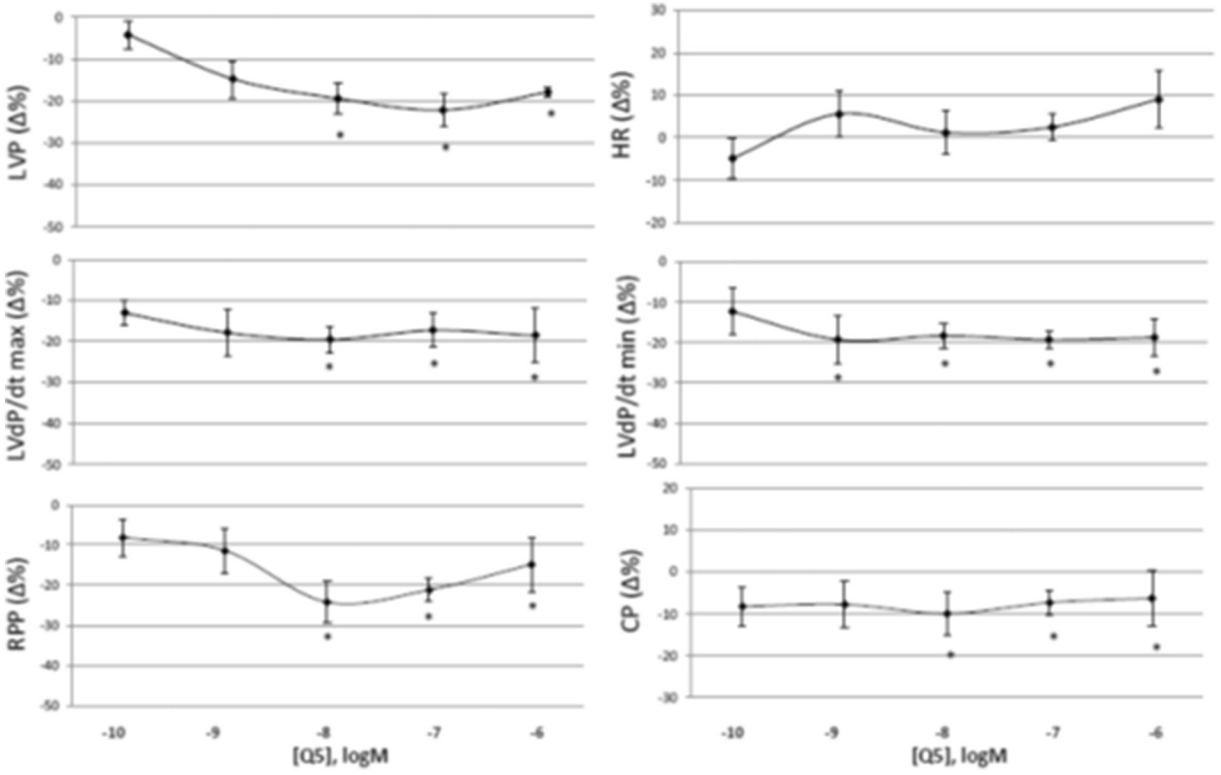

Fig. 7. Dose-dependent response curves of **Q5** (10^{-10} M–10^{-6} M) on LVP, HR, LVd*P*/d*T* max, LVd*P*/d*T* min, RPP and CP, on Langendorff perfused rat heart preparations. Percentage changes were evaluated as means ± SEM of 7 experiments. Significance of difference from control values was evaluated by one-way ANOVA; $P = 0 < 0.05$.

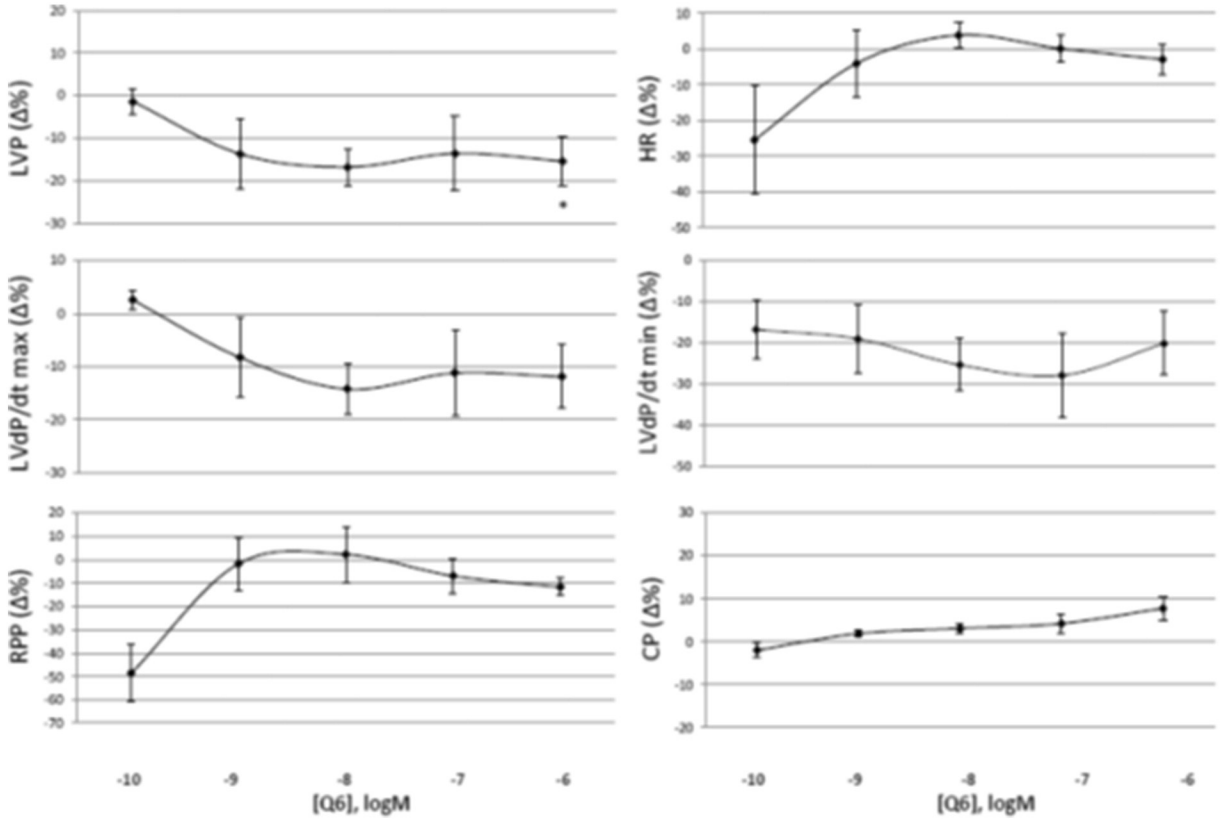

Fig. 8. Dose-dependent response curves of **Q6** (10^{-10} M–10^{-6} M) on LVP, HR, LV*d*P/d*T* max, LV*d*P/d*T* min, RPP and CP, on Langendorff perfused rat heart preparations. Percentage changes were evaluated as means ± SEM of 7 experiments. Significance of difference from control values was evaluated by one-way ANOVA; $P = 0 < 0.05$.

of hydroxyl groups (**Q5**) resulted in a more hydrophobic molecule than **Q1** (see Table 1 with clogP). Interestingly, the other substitutions that increased significantly the hydrophobicity of the analogs (**Q3**, **Q4** and **Q6**), not only might lead to very poorly soluble compounds (clogP >5), but they could also be rapidly hydrolysed in vivo.

For this reason, **Q5** derivative was selected for the evaluation of the in vitro bioavailability, according to the dialysis tubing procedure, a fast, reliable and low cost method, which allows to evaluate the bioavailability of different kinds of compounds. The test was conducted on **Q1** as well, used as control to compare bioavailability data.

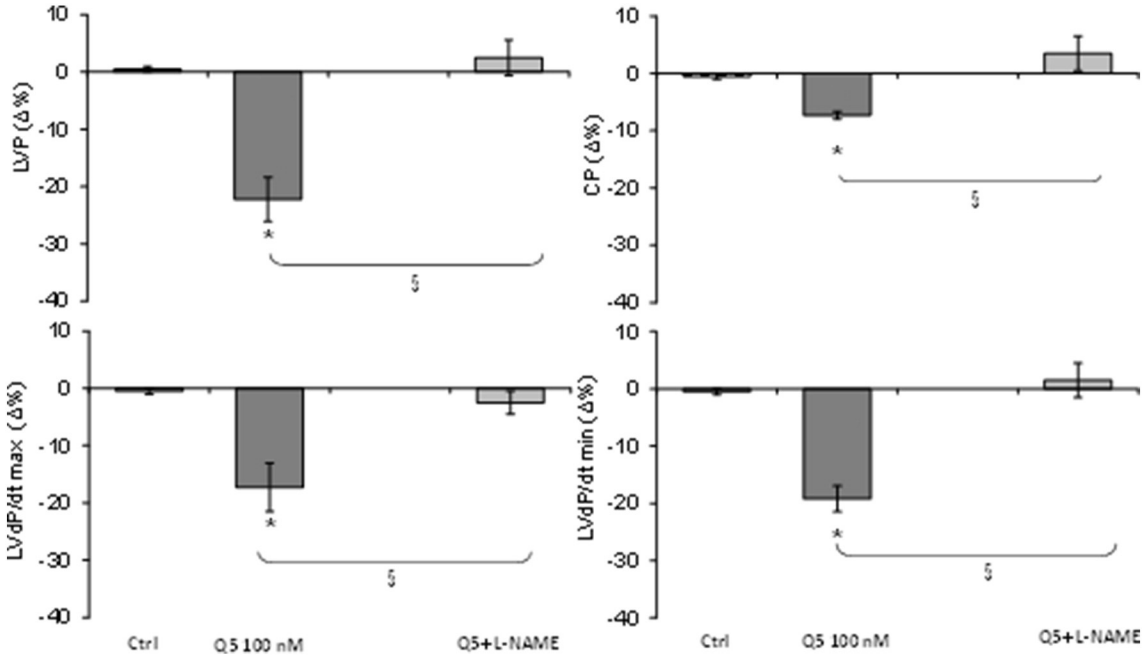

Fig. 9. Effects of **Q5** (100 nM) before and after treatment with the NOSs inhibitor L-NAME (10 μM) on LVP, LV*d*P/d*T* max, LV*d*P/d*T* min, and CP, on Langendorff perfused rat heart preparations. Percentage changes were evaluated as means ± SEM of 5 experiments. Significance of difference from control values was evaluated by t-test; $P = 0 < 0.05$.

Table 1
clogP (o/w) values of quercetin (**Q1**) and its synthetic derivatives (**Q2-Q6**).

Quercetin derivative	Weight	clogP (o/w)
Q1 (quercetin)	302.238	2.032
Q2	512.423	2.9887
Q3	466.445	6.5850
Q4	592.566	7.3080
Q5	442.508	4.8087
Q6	752.863	12.0437

Bioavailability is defined as the percentage of the tested molecule recovered in the bioaccessible fraction, after *in vitro* digestion, in relation to the original non-digested sample and it can be calculated by the following Eq. (1):

$$\text{Bioavailability}\ (\%) = \frac{\text{Bioaccessible content}}{\text{Total content}} \times 100 \quad (1)$$

The *in vitro* evaluation of the bioavailability of **Q5** has shown an enhanced bioaccessibility since the first 2 h (the obtained results were reported in Table 2), reaching almost 19% at the end of the experiment. On the other hand, according to our procedure, the bioavailability of unmodified quercetin (**Q1**) showed a total percentage slightly under 11%. This result suggests that improving lipophilicity by ethylation is important in increasing the amount of **Q1** that could potentially reach the bloodstream.

Previous studies reported data about *in vivo* bioavailability of **Q1**. Reinboth et al. (2010) reported a 4% absolute bioavailability of **Q1** in dogs, while the bioavailability of unchanged **Q1** in pigs is 0.54% (Ader et al., 2000). Also oral bioavailability evaluation in human volunteers has been conducted in the past, showing that less than 2% of orally administered **Q1** can be found in bloodstream (Gugler et al., 1975). Compared to these results, **Q5** displays a greatly improved bioavailability.

3.6. In vivo studies

Due to coronary dilation, the negative inotropism and lusitropism induced by **Q5**, this quercetin derivative (10 nM) was administrated to the rat for 1 month in the drinking water in order to analyze its anti-hypertensive properties. For this purpose, the spontaneous hypertensive rat (SHR) were used as models of human hypertensive condition, and Wistar Kyoto rats as normotensive control (n = 6 for each groups) (Harlan, Italy). Tail cuff method was used for weekly measures of systolic and diastolic blood pressure (BP). Tail cuff was connected to a pneumatic pulse transducer and a programmed electro-sphygmomanometer (BP-2000 series II; blood pressure analysis system, Visitech System). Blood pressures measured are reported in Table 3.

These data suggest that the chronic administration of the **Q5** determines a reduction of systolic and diastolic pressure in the presence of hypertension.

4. Conclusion

Poor bioavailability and low stability of quercetin could be determining factors of its beneficial effects; therefore, in the present research study, a small series (**Q2**–**Q6**) of variously substituted **Q1** derivatives was synthesized in the aim to overcome these limitations without affecting the cardioprotective properties of this polyphenol.

The best structural combination required for cardiovascular activity seems to be functional substitution of each OH group with an ethyl moiety (**Q5** derivative). Accordingly, among all the tested compounds, only this derivative determined a significant reduction of the left ventricular pressure (LVP), from 10^{-8} M to 10^{-6} M. This compound also increased relaxation and coronary dilation, and inotropism, lusitropism and coronary effects were abolished by NOSs inhibition by L-NAME. Furthermore, the chronic administration of higher doses of such a compound on SHR determined a significant reduction of systolic and diastolic pressure.

The acetyl derivative **Q2** instead, induced a negative inotropism and lusitropism significant at 10^{-10} M and from 10^{-8} to 10^{-6} M, while it did not modify the coronary pressure.

The obtained results suggest that the substitution of all OH groups present in **Q1** molecule with ethyl groups improves the bioavailability and stability of this flavonol. Moreover, the synthesized ethyl derivative **Q5** has been shown good antihypertensive properties; therefore, it could represent a good candidate for clinical use in the presence of hypertension and, thus, warrant further preclinical and mechanistic investigation.

Table 2
In vitro bioavailability (%) of **Q5** and **Q1** after pepsin (2 h) and pancreatin (4 h) digestions.

Time point	**Q5** bioavailability (%)	**Q1** bioavailability (%)
Pepsin digestion (2 h)	8.5 ± 0.7	4.4 ± 0.9
Pancreatin digestion (4 h)	10.3 ± 0.8	6.3 ± 0.8
Total *in vitro* bioavailability (6 h)	18.8 ± 1.2	10.7 ± 1.3

Table 3
Systolic and diastolic BP values measured in WKY and SHR before and after **Q5** administration. Significance of difference was evaluated by t-test.

	Systolic BP (mm Hg)		Diastolic BP (mm Hg)	
	Before **Q5**	After **Q5**	Before **Q5**	After **Q5**
WKY	120 ± 2.3	119 ± 2.5	83 ± 3.9	75 ± 3.3
SHR	197 ± 6.6	145 ± 7.0*	132 ± 6.3	101 ± 5.9*

* $P < 0.05$

Acknowledgments

This research work is financially supported under research project PON — SPREAD BIO OIL grant no. PON01_00293.

We also acknowledge the support of the Life Science Research Network Wales grant no. NRNPGSep14008, an initiative funded through the Welsh Government's Ser Cymru program.

References

Ader, P., Wessmann, A., Wolffram, S., 2000. Bioavailability and metabolism of the flavonol quercetin in the pig. Free Radic. Biol. Med. 28, 1056–1067.
Angelone, T., Caruso, A., Rochais, C., Caputo, A.M., Cerra, M.C., Dallemagne, P., Filice, E., Genest, D., Pasqua, T., Puoci, F., Saturnino, C., Sinicropi, M.S., El-Kashef, H., 2015. Indenopyrazole oxime ethers: synthesis and β 1-adrenergic blocking activity. Eur. J. Med. Chem. 92, 672–681.
Angelone, T., Pasqua, T., Di Majo, D., Quintieri, A.M., Filice, E., Amodio, N., Tota, B., Giammanco, M., Cerra, M.C., 2011. Distinct signalling mechanisms are involved in the dissimilar myocardial and coronary effects elicited by quercetin and myricetin, two red wine flavonols. Nutr. Metab. Cardiovasc. Dis. 21, 362–371.
Bhattaram, V.A., Graefe, U., Kohlert, C., Veit, M., Derendorf, H., 2002. Pharmacokinetics and bioavailability of herbal medicinal products. Phytomedicine 9 (Suppl. 3), 1–33.
Bouktaib, M., Lebrun, S., Atmanib, A., Rolando, C., 2002. Hemisynthesis of all the O-monomethylated analogues of quercetin including the major metabolites, through selective protection of phenolic functions. Tetrahedron 58, 10001–10009.
Brodde, O.E., Bruck, H., Leineweber, K., 2006. Cardiac adrenoceptors: physiological and pathophysiological relevance. J. Pharmacol. Sci. 100, 323–337.
Cai, X., Fang, Z., Dou, J., Yu, A., Zhai, G., 2013. Bioavailability of quercetin: problems and promises. Curr. Med. Chem. 20, 2572–2582.
Campiglia, P., Pezzi, V., 2013. Biological activity of 3-chloro-azetidin-2-one derivatives having interesting antiproliferative activity on human breast cancer cell lines. Bioorg. Med. Chem. Lett. 23, 6401–6405.
Carocci, A., Catalano, A., Bruno, C., Lentini, G., Franchini, C., De Bellis, M., De Luca, A., Conte Camerino, D., 2010. Synthesis and in vitro sodium channel blocking activity evaluation of novel homochiral mexiletine analogs. Chirality 22 (3), 299–307.
Catalano, A., Budriesi, R., Bruno, C., Di Mola, A., Defrenza, I., Cavalluzzi, M.M., Micucci, M., Carocci, A., Franchini, C., 2013. Searching for new antiarrhythmic agents: evaluation of meta-hydroxymexiletine enantiomers. Eur. J. Med. Chem. 65, 511–516.
Cherezov, V., Rosenbaum, D.M., Hanson, M.A., Rasmussen, S.G.F., Foon, S.T., Kobilka, T.S., Choi, H.-J., Kuhn, P., Weis, W.I., Kobilka, B.K., Stevens, R.C., 2007. High-resolution

crystal structure of an engineered human β_2-adrenergic G protein-coupled receptor. Science 318, 1258–1265.
Chimento, A., Sala, M., Gomez-Monterrey, I.M., Musella, S., Bertamino, A., Caruso, A., Sinicropi, M.S., Sirianni, R., Puoci, F., Parisi, O.I., Campana, C., Martire, E., Novellino, E., Saturnino, C., Conti, V., Russomanno, G., Corbi, G., Izzo, V., Vecchione, C., Filippelli, A., 2013. Adrenoreceptorsand nitric oxide in the cardiovascular system. Front. Physiol. 6, 4–321.
Deschner, E.E., Ruperto, J., Wong, G., Newmark, H.L., 1991. Quercetin and rutin as inhibitors of azoxymethanol-induced colonic neoplasia. Carcinogenesis 12, 1193–1196.
Duarte, J., Pérez-Palencia, R., Vargas, F., Ocete, M.A., Pérez-Vizcaino, F., Zarzuelo, A., et al., 2001. Antihypertensive effects of the flavonoid quercetin in spontaneously hypertensive rats. Br. J. Pharmacol. 133, 117–124.
Duarte, J., Pérez-Vizcaíno, F., Zarzuelo, A., Jiménez, J., Tamargo, J., 1993. Vasodilator effects of quercetin in isolated rat vascular smooth muscle. Eur. J. Pharmacol. 239, 1–7.
Ferry, D.R., Smith, A., Malkhandi, J., Fyfe, D.W., deTakats, P.G., Anderson, D., Baker, J., Kerr, D.J., 1996. Phase I clinical trial of the flavonoid quercetin: pharmacokinetics and evidence for in vivo tyrosine kinase inhibition. Clin. Cancer Res. 2, 659–668.
Gugler, R., Leschik, M., Dengler, H.J., 1975. Disposition of quercetin in man after single oral and intravenous doses. Eur. J. Clin. Pharmacol. 9, 229–234.
Hayek, T., Fuhrman, B., Vaya, J., Rosenblat, M., Belinky, P., Coleman, R., Elis, A., Aviram, M., 1997. Reduced progression of atherosclerosis in apolipoprotein E-deficient mice following consumption of red wine, or its polyphenols quercetin or catechin, is associated with reduced susceptibility of LDL to oxidation and aggregation. Arterioscler. Thromb. Vasc. Biol. 17, 2744–2752.
Kaur, C., Kapoor, H.C., 2001. Antioxidants in fruits and vegetables — the millennium's health. Int. J. Food Sci. Technol. 36, 703–725.
Kim, M.K., Park, K.S., Lee, C., Park, H.R., Choo, H., Chong, Y., 2010. Enhanced stability and intracellular accumulation of quercetin by protection of the chemically or metabolically susceptible hydroxyl groups with a pivaloxymethyl (POM) promoiety. J. Med. Chem. 53, 8597–8607.
Larson, A.J., Symons, J.D., Jalili, T., 2010. Quercetin: a treatment for hypertension?—a review of efficacy and mechanisms. Pharmaceuticals 3, 237–250.
Lu, C., Huang, F., Li, Z., Ma, J., Li, H., Fang, L., 2014. Synthesis and bioactivity of quercetin aspirinates. Bull. Kor. Chem. Soc. 35, 518–520.
Miller-Gallacher, J.L., Nehmé, R., Warne, T., Edwards, P.C., Schertler, G.F.X., Leslie, A.G.W., Tate, C.G., 2014. The 2.1 Å resolution structure of cyanopindolol-bound β_1-adrenoceptor identifies an intramembrane Na^+ ion that stabilises the ligand-free receptor. PLoS One 9, e92727.
Pereira, M.A., Grubbs, C.J., Barnes, L.H., Li, H., Olson, G.R., Eto, I., Juliana, M., Whitaker, L.M., Kelloff, G.J., Steele, V.E., Lubet, R.A., 1996. Effects of the phytochemicals, curcumin and quercetin, upon azoxymethane-induced colon cancer and 7,12-dimethylbenz[*a*]anthracene-induced mammary cancer in rats. Carcinogenesis 17, 1305–1311.
Pérez-Vizcaíno, F., Ibarra, M., Cogolludo, A.L., Duarte, J., Zaragozá-Arnáez, F., Moreno, L., López-López, G., Tamargo, J., 2002. Endothelium-independent vasodilator effects of the flavonoid quercetin and its methylated metabolites in rat conductance resistance arteries. J. Pharmacol. Exp. Ther. 302, 66–72.
Picq, M., Prigent, A.F., Ngmoz, G., Andrè, A.C., Pacheco, H., 1982. Pentasubstituted quercetin analogues as selective inhibitors of particulate 3′:5′-cyclic-AMP phosphodiesterase from rat brain. J. Med. Chem. 25, 1192–1198.
Pignatelli, P., Pulcinelli, F.M., Celestini, A., Lenti, L., Ghiselli, A., Gazzaniga, P.P., Violi, F., 2000. The flavonoids quercetin and catechin synergistically inhibit platelet function by antagonizing the intracellular production of hydrogen peroxide. Am. J. Clin. Nutr. 72, 1150–1155.
Reinboth, M., Wolffram, S., Abraham, G., Ungemach, F.R., Cermak, R., 2010. Oral bioavailability of quercetin from different quercetin glycosides in dogs. Br. J. Nutr. 104, 198–203.
Sharma, A., Gupta, H., 2010. Quercetin — a flavonoid. Chron. Young Sci. 1, 10–15.
Verma, A.K., Johnson, J.A., Gould, M.N., Tanner, M.A., 1988. Inhibition of 7,12-dimethylbenz(a)anthracene and N-nitrosomethylurea induced mammary cancer by dietary flavonol quercetin. Cancer Res. 48, 5754–5788.
Wallace, C.H.R., Baczko, I., Jones, L., Fercho, M., Light, P.E., 2006. Inhibition of cardiac voltage-gated sodium channels by grape polyphenols. Br. J. Pharmacol. 149 (6), 657–665.
Woo, A.Y., Xiao, R.P., 2002. Beta-adrenergic receptor subtype signaling in heart: from bench to bedside. Acta Pharmacol. Sin. 33, 335–341.